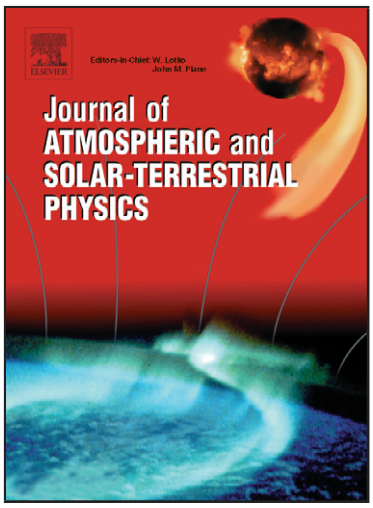

Peak characteristics of F2 region over Tucumán predictions and measurements

R.G. Ezquer, M. Mosert, L. Scidá, J. López

PII: S1364-6826(08)00099-0
DOI: doi:10.1016/j.jastp.2008.04.004
Reference: ATP 2715

Journal of Atmospheric and Solar–Terrestrial Physics

Received date: 9 May 2007
Revised date: 22 November 2007
Accepted date: 1 April 2008

Cite this article as: R.G. Ezquer, M. Mosert, L. Scidá and J. López, Peak characteristics of F2 region over Tucumán predictions and measurements, *Journal of Atmospheric and Solar–Terrestrial Physics* (2008), doi:10.1016/j.jastp.2008.04.004

1. Peak characteristics of F2 region over Tucumán. Predictions and measurements

2. R. G. Ezquer[a,b*,c], M. Mosert [c,d], L. Scidá[b] and J. López[a]

3. [a] CIASUR, Facultad Regional Tucumán, Universidad Tecnológica Nacional, Argentina

4. [b*] Laboratorio de Ionósfera, Dto. de Física, Universidad Nacional de Tucumán, Independencia 1800,

5. 4000 S. M. Tucumán, Argentina

6. [E-mail: rezquer@herrera.unt.edu.ar] – Fax : +54 381 4305401

7. [c] CONICET, Argentina

8. [d] CASLEO, Avda. España 1512-Sur, 5400 San Juan, Argentina

9. [E-mail: mmosert@casleo.gov.ar]

10. Abstract

11. Ionosonde measurements obtained at Tucumán are used to check the validity of the International
12. Reference Ionosphere model to predict the maximum electron density of F2 region (NmF2) and
13. its height (hmF2) over this station. Data corresponding to different months and solar activity
14. conditions are considered. CCIR and URSI options are used to model calculations. The results show
15. that, generally, the predictions of hmF2 are better than those of NmF2. Disagreements between
16. predicted and measured NmF2 values are observed and the consequence in the vertical total electron
17. content modeling are stressed.

18.

19. **Keywords:** ionosphere, electron density, height, modelling

20.

21. 1. Introduction

22. For successful radio communication, it is essential to predict the behavior of the ionospheric region
23. that will affect a given radio communication circuit. Such a prediction will identify the time periods,

the path regions and the sections of high frequency bands that will allow or disrupt the use of the selected high frequency communication circuit. This need for prediction leads to modeling of the ionosphere. Several models physical, empirical and semiempirical (e.g. Anderson, 1973; Bent et al., 1976; Llewellyn and Bent, 1973; Bilitza, 1990; Anderson et al., 1987; Ezquer et al, 1992; Ezquer et al, 1994) have been developed to predict ionospheric variables.

In a previous work Ezquer et al. (1996) used measurements of the critical frequencies of the ionospheric regions (foE, foF1 and foF2) obtained at South American stations for different solar conditions and seasons to check the validity of International Reference Ionosphere model (IRI) (Bilitza, 1990) to predict these frequencies. They found good predictions for foE and foF1 when compared. The degree of accuracy among experimental and predicted foF2 values was lower than those observed for the other frequencies, and cases with strong disagreements were observed by Ezquer et al. (1996).

Values of the F2 region maximum electron density height (hmF2) obtained from ground ionosonde data at South American latitudes were used by Ezquer et al (2003) to check the validity of the IRI to predict this variable. To this end they compared hmF2 predictions given by the model when ground ionosonde data were used as input parameter in the model ($hmF2_{IRI\text{-}Exp}$), against those obtained using the standard option ($hmF2_{IRI\text{-}CCIR}$). Their results suggest that, in general, the standard option of the model gives good hmF2 predictions at South American latitudes. Few cases showed deviation between 10% and 25%. The comparison with the results obtained by Ezquer et al. (1996) showed that the IRI performance in predicting hmF2 was better than in predicting foF2.

Deviations between IRI predictions and ionospheric measurements obtained near the southern crest of the equatorial anomaly were also observed by Ríos et al (2007). These authors considered data of only one year.

In order to advance in this study, in the present paper values of the maximum electron density of the F2 region (NmF2) and its height (hmF2) calculated from ground ionosonde data obtained at Tucumán (26.9° S, 294.6° E), station placed near de Southern peak of the equatorial anomaly, are used to check the validity of IRI to predict the peak characteristics of F2 region over Tucumán.

2. Data and results

The data were obtained at Tucumán during equinox and solstices. These data correspond to the low and high solar activity years 1965 and 1970, respectively, and also to the moderate solar activity years 1967 and 1972. In this work median is used as monthly value because it has the advantage of being less affected by large deviations in the value of the ionospheric characteristics that can occur during magnetic storm.

To obtain NmF2 we used the following equation:

$$NmF2 = 1.24 \times 10^4 \times foF2^2 \quad (1)$$

where NmF2 is in cm^{-3} and foF2 is the critical frequency of F2 region in Mhz.

For the worlwide description of the peak electron density, the International Radio Consultative Committee (CCIR) coefficients map (1967a, 1967b) and the URSI coefficients map (Rush et al, 1989) are used as choices in IRI model.

In this work CCIR and URSI choices are used in IRI to obtain modeled values of NmF2.

To obtain the experimental value of NmF2 we used measured foF2 in equation (1).

In the IRI model, hmF2 is obtained by its close correlation with the propagation parameter M(3000)F2 (Shimazaki, 1955; Bradley and Dudeney, 1973; Bilitza et al., 1979). M(3000)F2 is defined as

$$M(3000)F2 = MUF/foF2 \quad (2)$$

where MUF is the maximum usable frequency that, refracted in the ionosphere, can be received at a distance of 3000 km. This factor has been routinely scaled from ionograms, and numerical maps (CCIR, 1967a, 1967b) are used has a choice in the IRI model. The F2 peak height is calculated from

M(3000)F2 with the empirical formula (Bilitza et al. 1979)

$$hmF2 = 1490/[M(3000)F2 + DM] - 176 \quad (3)$$

where DM is a correction factor which depends on the critical frequencies of F2 and E regions, the 12-month running mean of solar sunspot number, and the magnetic dip latitude. In this paper we calculate hmF2 using the CCIR option in IRI and also using groung ionosonde measurements as input parameters in the model, from now on: $hmF2_{IRI\text{-}CCIR}$ and $hmF2_{IRI\text{-}Exp}$ values, respectively. We assume that $hmF2_{IRI\text{-}Exp}$ is a more realistic value of the maximum electron density height.

We consider $hmF2_{IRI\text{-}Exp}$ as the experimental value of hmF2 and $hmF2_{IRI\text{-}CCIR}$ as the modeled value of that height.

We calculated the deviation among modeled and experimental values as:

$$D\ \% = [(\text{modeled value} - \text{experimental value}) / (\text{experimental value})] \times 100 \quad (4)$$

The top panels of Figure 1 shows the results corresponding to the maximum electron density of the F2 region for June 1965, a low solar activity month. Good predictions are given by URSI option for nighttime hours. The greatest deviations among predictions and measurements are observed since 9 UT to 11 UT reaching values greater than 50%.

In general the predictions obtained with CCIR and URSI are similar.

The results for September 1965 are shown in the bottomside of Figure 1. The greatest disagreements among predictions and measurements are observed since 8 UT to 14 UT reaching values close to 50%.

Results for moderate solar activity are shown in Figure 2. For June 1967 it can be seen that the highest disagreement for CCIR option are observed for the period (4 UT, 7 UT) and high D% values are observed for daytime hours. For URSI the highest deviations are obtained for at hours of minimum ionization, with

values greater than 100%. Similar deviations are obtained with both options since 13 UT to 23 UT. For September 1967 a considerable underestimation is observed at 7 UT.

Figure 3 show results for high solar activiy months. For June 1970 similar deviations are obtained using both options since 13 UT to 19 UT. Disagreements greater than 50% are obtained with URSI options for hours of minimum ionization.

For September 1970, in general better predictions are obtained with CCIR.

The hmF2 results for the three considered solar activities are shown in Figure 4. It can be seen low deviation among modeled and experimental values. In general, deviations no greater than 10% are obtained.

Table 1 summarizes the results for NmF2 URSI option. The white cells correspond to the cases where the absolute value of the deviation among modeled and experimental values is lower than 30%. Grey cells show deviations between 30% and 50% and black ones correspond to cases with deviations greater than 50%.

Table 2 shows the results for the CCIR option. It can be seen that CCIR predictions are better than URSI ones. Moreover, the highest deviations obtained with CCIR correspond to nighttime hours, and those given by URSI correspond to hours of minimum ionization.

Table 3 summarizes the results for hmF2. There are no cases with deviation grater than 20%. 85% and 15% of the considered cases have deviation lower than 10% and deviation ranging from 10% to 20%, respectively.

Figure 5 shows the percentages of the considered cases with a given deviation for NmF2 and hmF2 values. It can be seen that hmF2 predictions are better than those corresponding to NmF2. These results suggest that the IRI performance in predicting M(3000)F2 factor and hmF2 is better in predicting foF2 for the considered station.

In the other hand, several models have been developed in order to describe the vertical electron density (N) distribution profile. For the Chapman layer the N-profile is given by:

$$N(z) = NmF2 \exp\{0.5[1-z-\exp(-z)]\} \quad (5)$$

where z = (h-hm)/H is the normalized height measured from hmF2 in units of the scale height H. Chiu (1975) empirical model assumes that the N-profile in the F region can be expressed by two standard Chapman profile expressions, one for the bottomside profile and the other for the topside. They are

$$N(z) = NmF2 \exp [1-z_{lo}-\exp(-z_{lo})] \quad (6)$$

$$N(z) = NmF2 \exp [1-z_{up}-\exp(-z_{up})] \quad (7)$$

where the subscripts lo and up refer, respectively to the bottomside and topside profiles. Anderson (1987) developed a semiempirical low-latitude ionospheric model to obtain the F region N-profile. This model assumes the following modified Chapman expressions:

$$N(z) = NmF2 \exp\{C_{up} [1-z_{up}-\exp(-z_{up})]\} \quad (8)$$

$$N(z) = NmF2 \exp\{C_{lo} [1-z_{lo}-\exp(-z_{lo})]\} \quad (9)$$

In the Base Point Model (Ezquer et al., 1992), as in the Chiu (1975) and Anderson (1987) models, two Chapman profile expressions are assumed to describe the entire N-profile. They are

$$N(z) = NmF2 \exp [1-z_{up}-\exp(-z_{up})] \quad (10)$$

$$N(z) = NmF2 \exp\{0.5 [1-z_{lo}-\exp(-z_{lo})]\} \quad (11)$$

135. Reinisch et al (2004) also asume a Chapman function for the topside.

136. To model VTEC using the mentioned models, the following integral must be calculated

137. $$VTEC = \int NmF2 \, . \exp\{C\,[1-z-\exp(-z)]\}\, dz \qquad (12)$$

138. which can be expressed as

139. $$VTEC = NmF2 \int \exp\{C\,[1-z-\exp(-z)]\}\, dz \qquad (13)$$

140. or

141. $$VTEC = NmF2 \; SF(h) \qquad (14)$$

142. where SF(h) is a shape factor.

143. According to Eq.(14), the deviation between calculated and measured VTEC would be

144. $$D\%VTEC = D\%NmF2 + D\%SF(h) \qquad (15)$$

145. So, when the described expressions are used for VTEC calculations, the observed disagreements between

146. predictions and measurements could arise because NmF2 or shape of the N profile, or both, are not well

147. predicted.

148. Taking into account that the results of this work show that for Tucumán there are cases with NmF2

149. deviations equal to 40%, during daytime conditions, in the case that CCIR or URSI options are used to

150. model NmF2, for those cases would be possible that

151. D%VTEC > 40%. (16)

152. 3. Conclusions

153. The validity of the International Reference Ionosphere model to predict the maximum electron density of
154. the F2 region (NmF2) and its height (hmF2) over Tucumán, has been checked.
155. For NmF2, deviation as high as 50 % has been observed.
156. In general, the predictions of hmF2 are better than those of NmF2. These results suggest that the IRI
157. performance in predicting M(3000)F2 factor and hmF2 is better in predicting foF2 for the considered
158. station.
159. The consequence of D%NmF2 on the VTEC calculation has been stressed. It was shown that errors
160. greater than 40% could be produced in VTEC calculation for daytime condition, when NmF2
161. prediction is used as an input coefficient in a VTEC model.

162. References

163. Anderson, D.N., 1973. A theoretical study of the ionospheric F-region equatorial anomaly, II, Results in
164. the American and Asian sectors. Planet. Space Sci. 21, 421-428.

165. Anderson, D.N., Mendillo, M., Hertniter, B., 1987. A semiempirical low latitude ionospheric model.
166. Radio Sci. 22, 292-306.

167. Bent, R.B., Llewelyn, S.K., Nesterczuk, G., Schmid, P.E., 1976. The development of highly successful
168. worldwide empirical ionospheric model its use in certain areas of space communications and world
169. wide total electron content investigations. Goodman, J. (Ed.). Effect of the Ionosphere on Space
170. Systems and Communications. Springfield, VA, 13-28.

171. Bilitza D., 1990. International Reference Ionosphere, Report NSSDC/WDC-A-R&S 90-22. National Space
172. Science Data Center / World Data A for Rockets and Satellites, 43-77.

173. Bilitza D., Sheik N. M., Eyfrig R., 1979. A global model for the height of the F2-peak using values
174. from the CCIR. *Telecommun*. J. 46, 549-553.

175. Bradley, P. A., Dudeney, J. R., 1973. Vertical distrbuion of electron concentration in the
176. ionosphere. J. Atmos. Terr. Phys. 35, 2131-2146.

177. Chiu, Y.T., 1975. An improved phenomenological model of ionospheric density. J. Atmos. Terr. Phys.
178. 37, 1563-1570.

179. Ezquer, R.G., de Adler N.O., Radicella S.M., Gonzalez M.M., Manzano, J.R., 1992. Total electron
180. content obtained from ionogram data alone. Radio Sci. 27, 429-434.

181. Ezquer, R.G., de Adler N.O., Heredia T., 1994. Predicted and measured total electron content at both
182. peaks of the equatorial anomaly. Radio Sci. 29, 831-838.

183. Ezquer, R.G., Oviedo R. Del V., Jadur, C.A., 1996. Ionospheric predictions for South American
184. latitudes. Radio Sci. 31, 381-388.

185. Ezquer, R.G., Scidá, L., Mansilla. G.A., Mosert M., Herrera M.F., 2003. F2 region maximun electron
186. density height predictions for South American latitudes. Radio Sci. 38, 1076,
187. doi: 10.1029/2002RS002756, 15.1-15.11.

188. Iternational Radio Consultatve Committee (CCIR), Atlas of ionospheric characteristics, *Rep. 340*,
189. Int. Telecommun. Union, Geneva, 1967a.

190. Iternational Radio Consultatve Committee (CCIR), Atlas of ionospheric characteristics, *Rep. 340-2*
191. *(and later suppl.)*, Int. Telecommun. Union, Geneva, 1967a.

192. Llewellyn, S.K., Bent, R.B., 1973. Documentation and Description of the Bent ionospheric model,
193. AFCRL-TR-73-0657, AD 772733.

194. Reinisch, B.W., Huang, X.Q., Belehaki, A., et al., 2004. Modeling the IRI topside profile using scale
195. heights from ground-based ionosonde measurements, Adv. Space Res. 34, doi: 10.1016/j.asr.2004.06.012,
196. 2026-2031.

197. Rios, V.H., Medina C. F., Alvarez P., 2007. Comparison between IRI predictions and digisonde
198. measurements at Tucumán. J. Atmos. Solar-Terr. Phys. 69, 569-577.

199. Shimazaki, T., 1955. Worldwide daily variability in the height of the maximum electron density
200. of the ionospheric F2-layer. J. Radio Res. Lab. Jpn. *2*, 85-97.

201. FIGURES (Legends)

202. Fig 1. Modeled and experimental NmF2, in cm^{-3}, and Deviation. Experimental NmF2 was
203. calculated using hourly monthly median values of foF2 measured at Tucumán. Low solar
204. activity year 1965

205. Fig 2. Modeled and experimental NmF2, in cm^{-3}, and Deviation. Experimental NmF2 was
206. calculated using hourly monthly median values of foF2 measured at Tucumán. Moderate solar
207. activity year 1967

208. Fig 3. Modeled and experimental NmF2, in cm^{-3}, and Deviation. Experimental NmF2 was
209. calculated using hourly monthly median values of foF2 measured at Tucumán. High solar
210. activity year 1970

211. Fig 4. Deviation of hmF2 for low (1965), moderate (1967) and high (1970) solar activity

212. Fig 5. Percentages of all considered cases with a given deviation for NmF2 and hmF2

Table 1. Deviation (%) among modeled and experimental NmF2 values. URSI option

TUCUMAN - URSI

1965			
UT	JUNE	SEPT.	DECEMB.
0	5.64	-10.58	-
1	1.12	-2.60	-
2	9.02	-2.26	-
3	0.76	23.77	-
4	12.50	0.90	-
5	-4.40	4.42	-
6	3.62	3.04	-
7	-19.41	7.64	-
8	-40.76	24.04	37.94
9	-6.92	28.09	30.85
10	78.86	84.18	34.71
11	85.90	39.15	42.16
12	17.09	53.47	33.63
13	27.35	50.88	49.14
14	15.30	40.49	38.05
15	23.05	11.48	37.34
16	19.23	-0.85	25.36
17	-11.86	-1.35	12.90
18	-14.12	11.04	21.47
19	-8.16	-6.25	16.80
20	-13.73	-0.40	6.30
21	-25.94	-11.44	1.67
22	-38.87	-5.05	13.67
23	-	-13.47	14.69

1967				
UT	MARCH	JUNE	SEPT.	DECEMB
0	-	12.85	-	-
1	-	12.68	-	-
2	-	16.02	-	-
3	-	8.48	-	8.16
4	-	10.85	-	-5.39
5	-	21.45	-47.47	-17.84
6	-	22.44	-	-16.52
7	-	6.22	-49.36	-9.77
8	-44.97	-30.87	-25.20	-2.36
9	-20.61	42.58	-19.94	5.20
10	43.12	123.41	6.97	7.49
11	-14.79	121.08	12.69	5.95
12	-1.10	48.30	16.53	17.79
13	9.34	49.95	5.21	10.31
14	6.14	39.85	-6.08	3.60
15	-3.21	34.32	-5.75	7.73
16	-11.56	28.36	-12.62	0.71
17	-11.91	-0.67	-17.32	-6.23
18	-	5.74	-15.98	-9.19
19	-	3.57	-	-11.77
20	-	3.58	-	-11.73
21	-	-19.90	-	-14.00
22	-	-10.61	-	-
23	-	6.07	-	-

1970			
UT	JUNE	SEPT.	DECEMB.
0	-	-	-
1	-	-	-
2	-	-	-
3	-22.17	-	-
4	-19.66	-	-
5	-13.54	-48.43	-5.65
6	-18.34	-	2.42
7	-37.56	-24.43	10.28
8	-41.09	7.91	-9.97
9	-8.75	33.08	-5.49
10	86.75	55.31	-2.25
11	72.12	30.02	15.05
12	3.95	12.48	24.56
13	-0.27	18.12	21.10
14	-13.13	11.51	10.62
15	-15.45	0.88	4.52
16	-17.18	-9.74	-0.52
17	-27.21	-14.85	-8.75
18	-24.80	-13.58	-15.42
19	-16.11	-	-17.65
20	-	-	-20.05
21	-	-	-14.79
22	-	-	-12.08
23	-	-	-6.47

1972				
UT	MARCH	JUNE	SEPT.	DECEMB.
0	-	-7.82	-43.52	-
1	-	-2.31	-44.08	4.86
2	-45.58	-4.84	-44.44	11.58
3	-46.03	-5.33	-37.51	28.87
4	-46.87	14.01	-39.33	8.25
5	-47.18	12.36	-44.75	-
6	-48.24	-8.53	-37.15	-
7	-57.37	-11.47	-23.56	-
8	-25.43	-30.06	-7.15	33.50
9	-14.20	9.68	5.70	75.10
10	43.51	109.09	56.67	18.41
11	-4.53	120.27	19.39	27.13
12	-10.28	13.24	4.35	19.90
13	1.15	10.96	-7.53	11.40
14	9.64	-2.55	-14.26	13.45
15	-5.28	-2.73	-13.24	17.33
16	-15.48	-10.83	-13.85	-0.19
17	-19.59	-17.22	-17.46	-10.00
18	-24.36	-14.84	-23.96	-10.09
19	-27.93	-10.66	-23.23	-22.60
20	-39.03	-14.06	-23.42	-28.23
21	-39.72	-23.85	-28.27	-28.58
22	-37.69	-26.02	-35.09	-
23	-38.56	-6.83	-34.67	-

White cells: |D%| ≤ 30% **Grey cells: 30% ≤ |D %| ≤ 50%** **Black cells: |D %| > 50%.**

Table 2. Deviation (%) among modeled and experimental NmF2 values. CCIR option

TUCUMAN - CCIR

1965			
UT	JUNE	SEPT.	DECEMB.
0	28.03	-3.13	-
1	28.48	6.85	-
2	34.92	8.69	-
3	21.24	41.19	-
4	34.41	17.31	-
5	12.84	17.96	-
6	24.67	8.00	-
7	0.65	2.06	-
8	-36.60	-0.40	27.93
9	-44.05	-17.14	14.18
10	-26.64	15.53	10.12
11	3.59	0.42	18.77
12	-7.95	26.58	20.36
13	18.63	33.47	39.35
14	13.31	29.13	25.41
15	22.96	7.90	21.28
16	19.08	1.05	13.65
17	-14.02	1.71	8.31
18	-17.01	12.45	21.12
19	-7.58	-4.96	17.11
20	-8.66	4.33	4.59
21	-20.81	-4.59	-2.98
22	-35.40	2.52	6.00
23	-	-7.01	7.16

1967				
UT	MARCH	JUNE	SEPT.	DECEMB
0	-	25.00	-	-
1	-	28.00	-	-
2	-	30.83	-	-
3	-	26.16	-	14.82
4	-	38.19	-	7.98
5	-	57.87	-30.04	-7.05
6	-	61.86	-	-13.40
7	-	43.84	-41.87	-13.85
8	-30.16	-16.47	-24.49	-10.98
9	-17.95	4.61	-35.62	-11.05
10	21.64	6.80	-23.54	-17.44
11	-29.69	28.85	-13.26	-19.21
12	-16.00	17.90	-1.28	-2.65
13	-6.26	39.86	-7.45	-2.66
14	-9.53	35.86	-16.47	-9.45
15	-16.33	31.25	-12.91	-8.95
16	-20.17	25.39	-14.89	-13.34
17	-16.86	-5.50	-18.08	-14.60
18	-	-2.20	-18.24	-14.34
19	-	-2.38	-	-17.12
20	-	2.06	-	-18.32
21	-	-19.85	-	-21.02
22	-	-10.91	-	-
23	-	9.71	-	-

1970			
UT	JUNE	SEPT.	DECEMB.
0	-	-	-
1	-	-	-
2	-	-	-
3	-9.48	-	-
4	0.16	-	-
5	12.39	-30.86	6.87
6	7.95	-	6.26
7	-15.45	-12.53	5.32
8	-28.82	10.07	-17.84
9	-33.05	8.08	-19.96
10	-10.72	11.68	-24.65
11	0.31	0.38	-11.78
12	-17.36	-4.57	3.47
13	-6.98	3.89	7.26
14	-15.61	-0.97	-3.07
15	-17.39	-7.00	-11.42
16	-19.09	-12.30	-14.11
17	-30.74	-15.83	-16.63
18	-30.45	-16.09	-19.92
19	-20.93	-	-22.30
20	-	-	-25.72
21	-	-	-21.56
22	-	-	-19.73
23	-	-	-15.44

1972				
UT	MARCH	JUNE	SEPT.	DECEMB.
0	-	3.58	-39.43	-
1	-	12.90	-39.00	-1.35
2	-37.65	8.79	-36.87	10.28
3	-33.60	10.66	-23.61	38.86
4	-31.32	41.35	-21.47	25.34
5	-29.82	44.05	-29.54	-
6	-29.75	19.20	-25.45	-
7	-41.64	18.37	-16.85	-
8	-4.62	-17.19	-12.17	22.52
9	-11.74	-22.24	-20.20	50.03
10	21.09	-2.71	7.68	-6.36
11	-21.11	27.25	-9.91	1.30
12	-23.23	-10.23	-12.36	3.28
13	-12.43	3.40	-18.58	1.10
14	-5.58	-5.19	-23.05	1.09
15	-17.34	-4.60	-18.72	1.34
16	-23.16	-12.52	-14.89	-11.83
17	-23.79	-20.88	-17.16	-15.82
18	-26.69	-20.58	-25.04	-12.72
19	-29.43	-14.70	-24.55	-24.83
20	-39.28	-14.09	-22.84	-31.51
21	-38.52	-22.81	-25.89	-33.18
22	-35.40	-25.48	-32.15	-
23	-36.24	-2.61	-30.96	-

White cells: |D%| ≤ 30% **Grey cells: 30% ≤ |D %| ≤ 50%** **Black cells: |D %| > 50%.**

Table 3. Deviation (%) among modeled and experimental hmF2 values.

1965			
UT	JUNE	SEPT.	DECEMB
0	-6.06	-0.97	1.68
1	-11.02	-3.82	-3.01
3	-9.95	-8.72	-15.39
4	-8.34	-12.15	-
5	-16.16	-15.34	-5.68
6	-14.11	-16.28	8.58
7	-8.45	4.16	3.64
8	-0.30	-8.32	-11.92
9	-1.33	-13.19	0.22
10	-11.59	-11.85	9.42
11	-8.54	2.69	-2.34
12	3.90	0.80	0.92
13	3.27	-6.02	0.68
14	0.24	-4.98	-2.84
15	4.47	1.15	-1.45
16	-0.75	5.06	1.01
17	1.70	6.03	7.61
18	0.81	-4.77	3.84
19	-7.02	-5.77	-4.90
20	-0.63	-2.02	0.68
21	-2.14	6.40	0.92
22	2.96	4.30	3.65
23	8.78	3.22	0.79

1967				
UT	MARCH	JUNE	SEPT.	DECEMB
0	7.74	-1.47	-6.89	-4.55
1	-	-7.15	-12.33	-0.71
3	10.66	2.74	-3.87	-1.13
4	-0.98	-1.69	-13.41	-12.28
5	-1.25	-6.57	-16.38	-6.05
6	1.49	-7.19	-7.22	-6.95
7	-2.59	-7.82	10.97	-6.74
8	4.23	7.04	-1.63	-2.70
9	-6.03	1.82	-1.46	-5.07
10	-13.18	-8.92	-4.60	-1.28
11	-1.78	-6.68	1.11	-3.71
12	-1.41	4.95	-5.51	-1.90
13	-1.09	-1.25	-7.68	-3.79
14	-2.65	6.09	-6.34	2.68
15	0.13	1.47	-4.20	4.49
16	4.32	7.50	1.09	7.98
17	3.81	5.66	-1.97	4.38
18	0.58	5.12	3.07	6.88
19	-2.75	2.09	-3.41	4.06
20	-4.89	-0.71	5.93	0.95
21	-	3.23	10.34	-1.69
22	4.41	8.81	9.47	-7.21
23	5.58	9.25	-1.74	-4.31

1970			
UT	JUNE	SEPT.	DECEMB
0	-6.19	6.73	-8.80
1	0.37	-1.97	-4.76
3	7.97	1.46	-9.61
4	0.51	-3.72	-5.35
5	-7.07	5.46	-6.72
6	-2.94	2.89	-2.61
7	1.48	8.55	-4.92
8	9.43	-3.84	-3.38
9	-0.78	-6.10	1.89
10	-9.04	-6.70	5.81
11	-4.57	3.98	3.48
12	1.96	2.12	-9.58
13	0.59	-0.09	-8.74
14	-1.93	1.42	-2.49
15	6.31	-1.33	4.74
16	-0.37	1.53	5.14
17	0.50	3.81	1.48
18	2.62	3.52	1.06
19	2.26	4.97	0.84
20	-2.97	9.18	0.10
21	6.18	13.72	-2.99
22	6.53	12.86	-6.33
23	18.01	9.63	-6.16

1972				
UT	MARCH	JUNE	SEPT.	DECEMB
0	-7.34	-5.42	-9.82	-0.69
1	-2.70	-6.07	-4.39	-3.66
3	-0.93	-0.90	-8.03	-7.47
4	-9.00	-9.63	-12.19	-15.44
5	-2.02	-13.86	-10.78	-9.67
6	0.53	-12.07	-6.55	-10.59
7	6.31	-8.20	0.62	-5.51
8	-2.37	3.57	-11.32	-6.42
9	-7.60	-6.56	-11.37	-13.30
10	-10.14	-16.57	-14.29	5.13
11	-0.88	-11.95	-4.42	-1.85
12	2.24	1.95	-6.13	-9.09
13	2.80	-1.57	-3.52	-5.18
14	1.40	-1.84	-2.25	1.48
15	-1.00	3.19	2.14	3.06
16	2.89	3.73	-0.81	5.93
17	-0.53	-3.26	-1.76	7.46
18	-6.37	-3.88	-4.72	3.96
19	-7.20	-6.69	-5.80	5.99
20	-1.98	-4.67	-4.46	7.21
21	1.99	4.02	-	3.05
22	1.93	4.32	0.48	1.44
23	-1.93	2.23	-5.25	-1.15

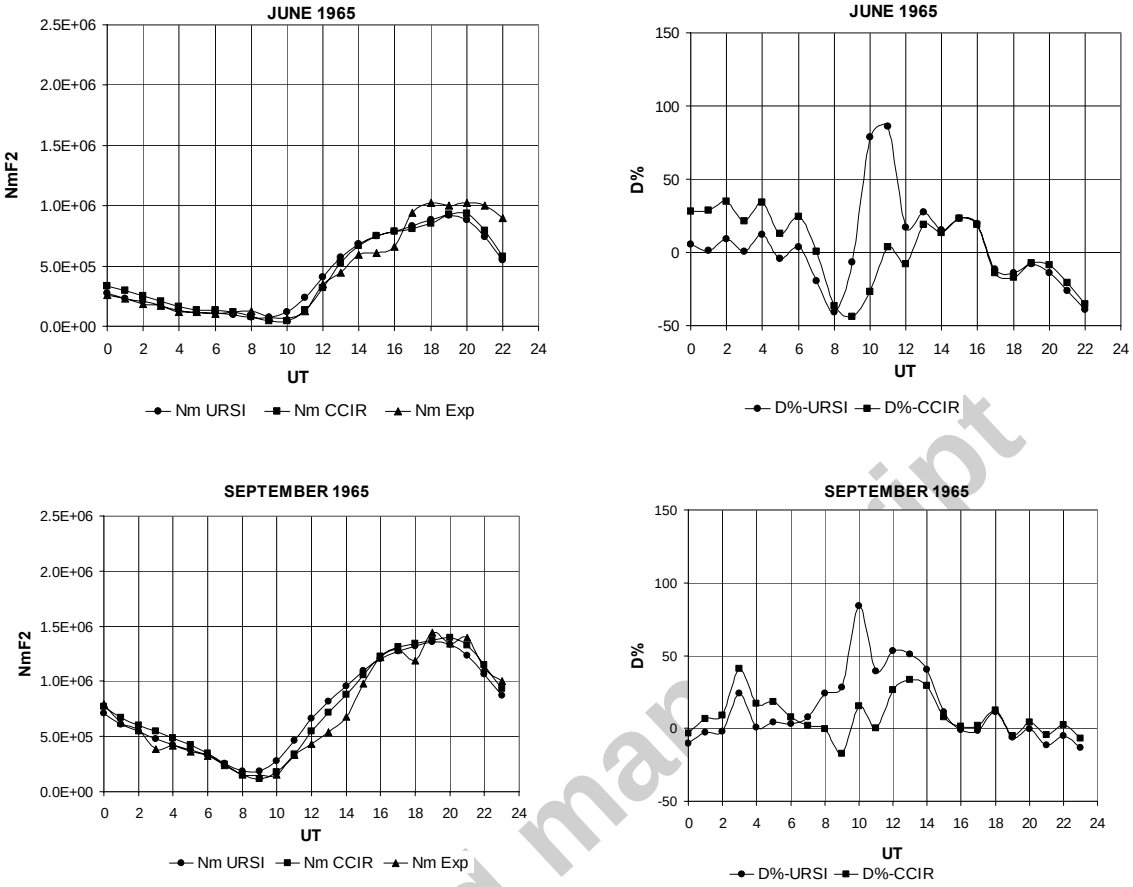

Fig 1.

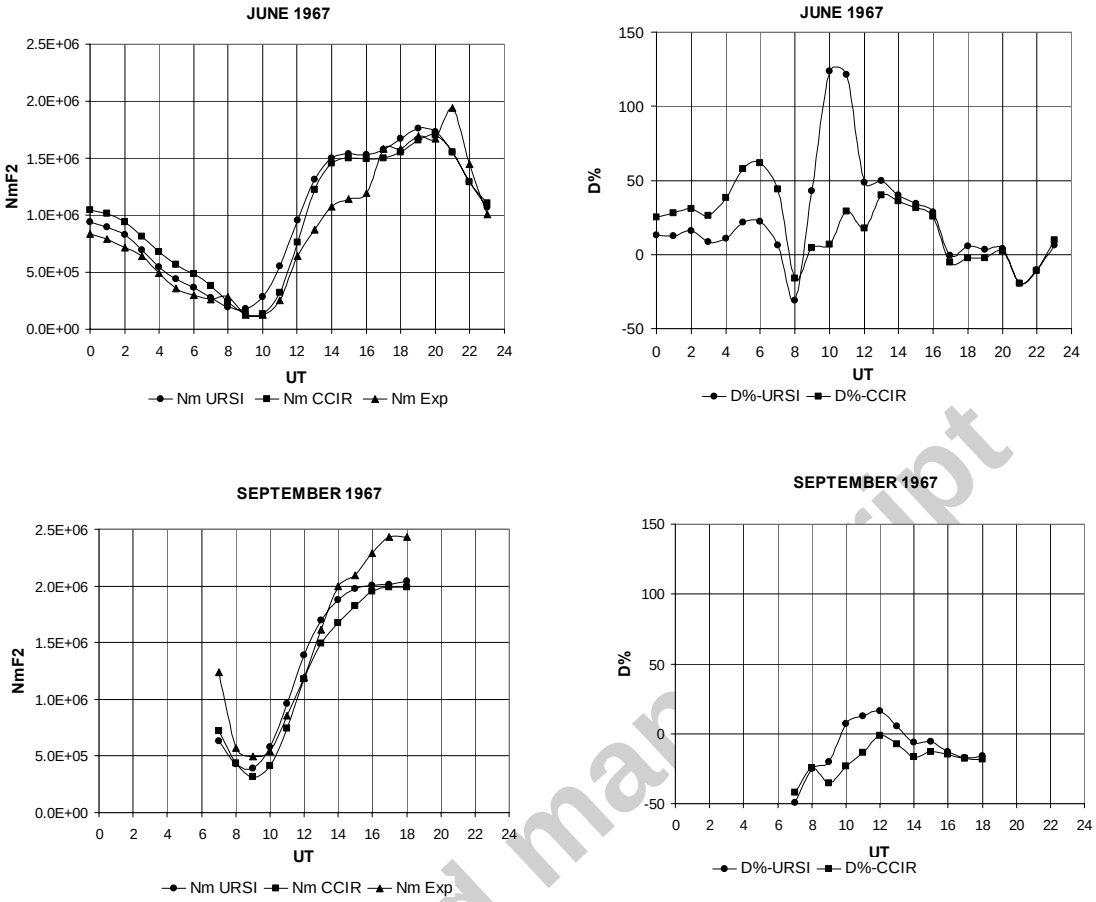

Fig 2.

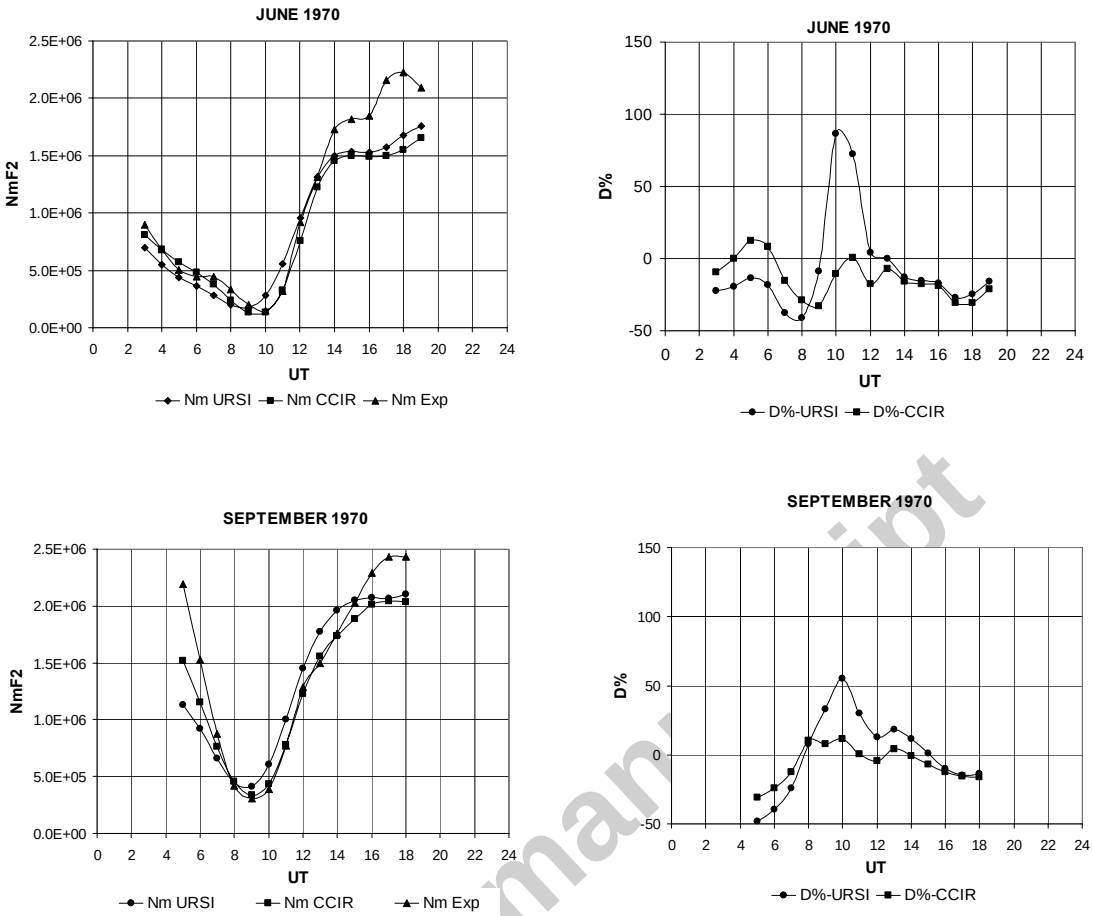

Fig 3

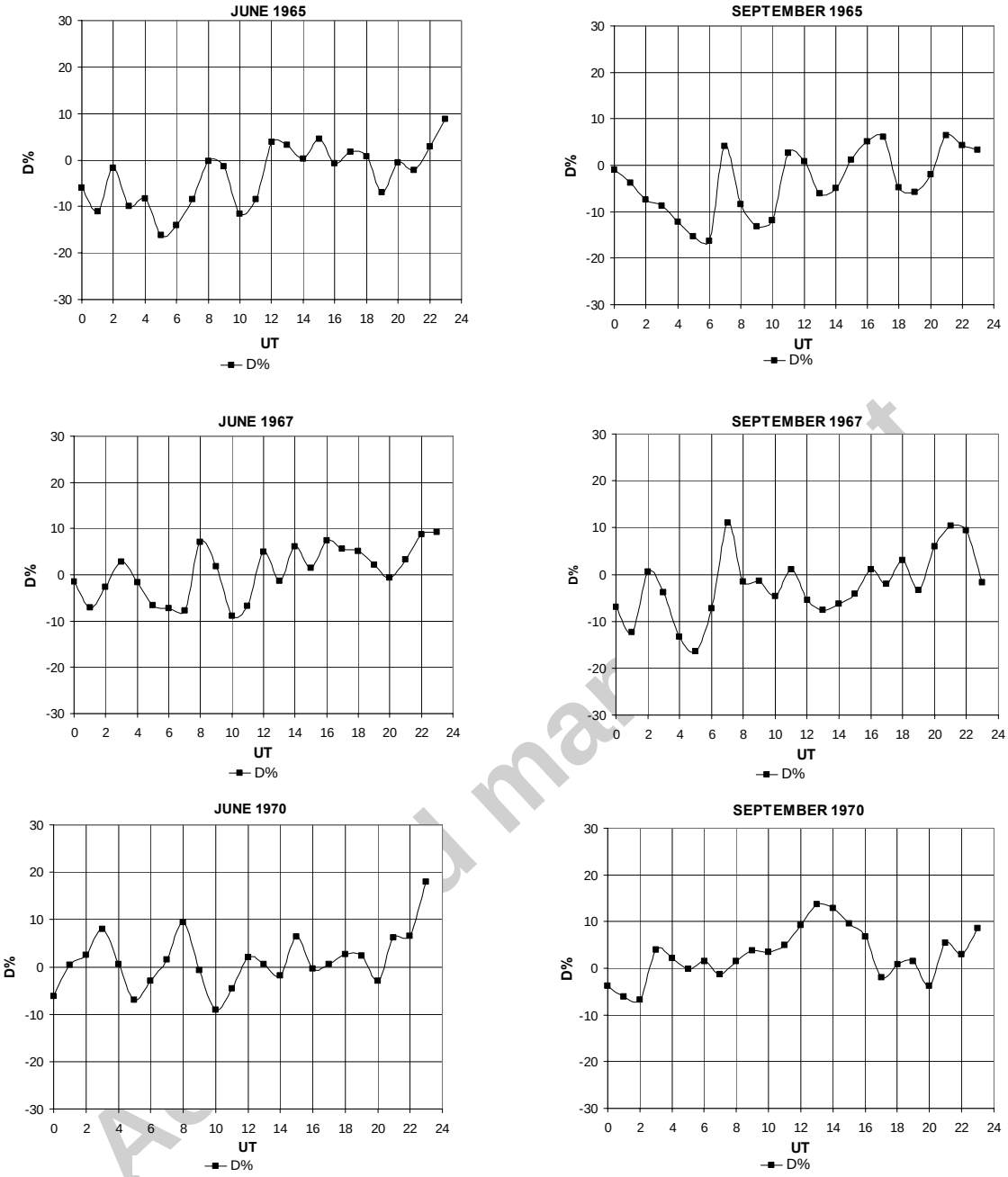

Fig 4.

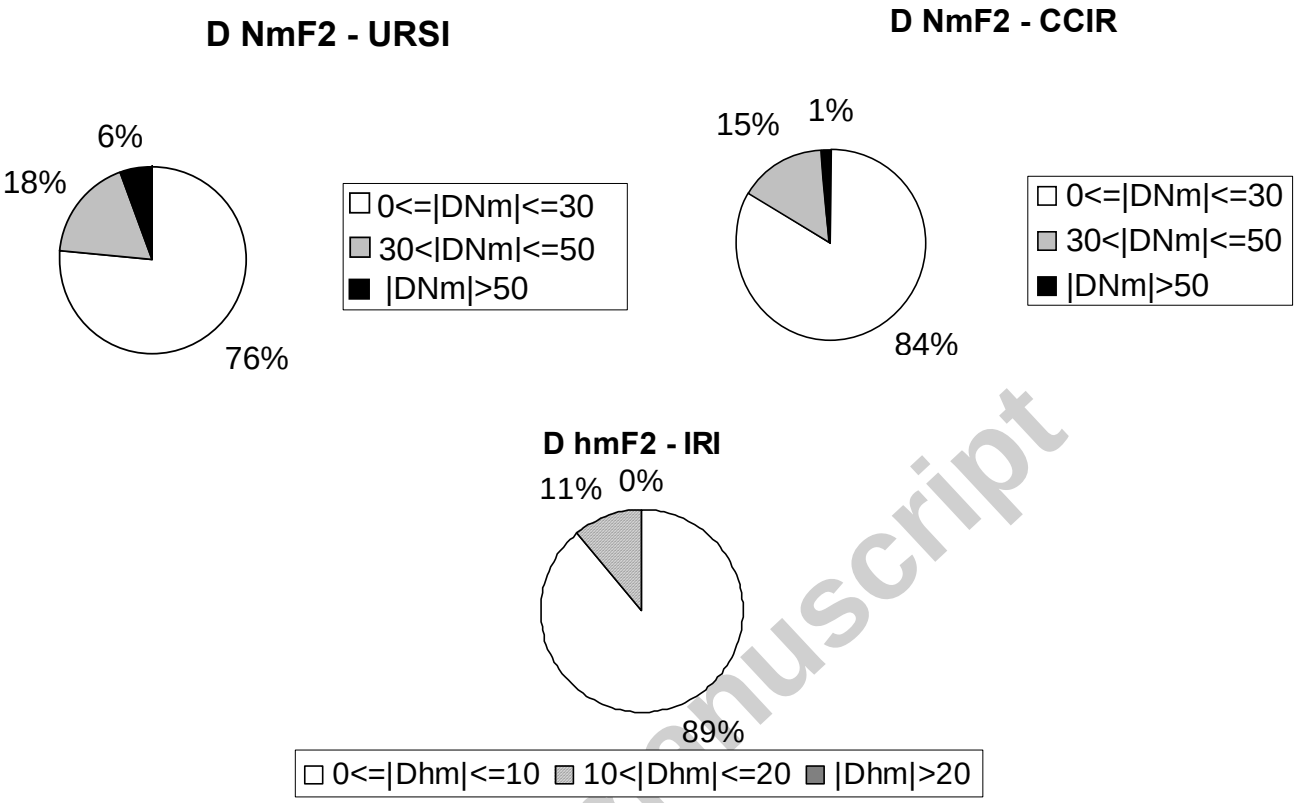

Fig 5